Surface tension effects on the behaviour of a rising bubble driven by buoyancy force*

Wang Han(王 含)[a], Zhang Zhen-Yu(张振宇)[b],
Yang Yong-Ming(杨永明)[a]†, and Zhang Hui-Sheng(张慧生)[a]

[a] *Department of Mechanics and Engineering Science, Fudan University, Shanghai* 200433, *China*
[b] *Department of Mathematics, Shanghai University of Finance and Economics, Shanghai* 200433, *China*

(Received 24 March 2009; revised manuscript received 18 June 2009)

In the inviscid and incompressible fluid flow regime, surface tension effects on the behaviour of an initially spherical buoyancy-driven bubble rising in an infinite and initially stationary liquid are investigated numerically by a volume of fluid (VOF) method. The ratio of the gas density to the liquid density is 0.001, which is close to the case of an air bubble rising in water. It is found by numerical experiment that there exist four critical Weber numbers We_1, We_2, We_3 and We_4, which distinguish five different kinds of bubble behaviours. It is also found that when $1 \leq We < We_2$, the bubble will finally reach a steady shape, and in this case after it rises acceleratedly for a moment, it will rise with an almost constant speed, and the lower the Weber number is, the higher the speed is. When $We > We_2$, the bubble will not reach a steady shape, and in this case it will not rise with a constant speed. The mechanism of the above phenomena has been analysed theoretically and numerically.

Keywords: rising bubble, surface tension, buoyancy, volume of fluid (VOF) method

PACC: 6810

1. Introduction

Multifluid systems play an important role in many natural and industrial processes such as combustion, petroleum refining, chemical engineering and cleaning. The rising of a buoyancy-driving bubble in a liquid is one of the typical multifluid systems. A sound understanding of the fundamentals of the rising bubble is crucial in a variety of practical applications ranging from the rise of steam in boiler tubes to gas bubbles in oil wells. It is difficult to study the mechanism of the bubble behaviour through a purely theoretical method because of the strong nonlinearity accompanied by large bubble deformations. As a result, approximate theoretical solutions have been obtained in the limit of very small bubble deformations for either high[1] or low[2] Reynolds numbers. The well-known analysis in Ref. [3] related the rising speed to the radius of curvature of the bubble at the forward stagnation point, but the overall spherical-cap shape was assumed *a priori* rather than determined as a part of a full solution.

Up to now, the large deformations of the bubble are studied mainly by experimental method and numerical simulation. Experimental method is the most direct and original approach for finding the new phenomena and exploring the associated mechanisms. Early observation works have been done by many researchers.[4−7] However, it is rather difficult to measure the flow pattern and pressure distribution within the bubble and its surrounding liquid while it is rising and deforming. Moreover, the correlations obtained by experiments are based on a limited number of liquid/gas systems. On the other hand, numerical methods can overcome these drawbacks and provide an effective and convenient way to solve multifluid flow problems.

The numerical simulation methods for multifluid problems can mainly be divided into two categories. One is the kind of boundary integral methods,[8] which only need to arrange the grids on the bubble surfaces and thus reduce the dimensions of the problem by one, so that the computational amounts are, compared to the other kind of methods mentioned below, reduced considerably. These methods can simulate the bubble shape with high resolution and can easily implement the simulation of surface tension effects accurately. The boundary conditions of the flow field at infinity can be satisfied exactly by these methods. However, this kind of method is difficult for simulating the topo-

*Project supported by the National Natural Science Foundation of China (Grant Nos. 10672043 and 10272032).
†Corresponding author. E-mail: yangym@fudan.edu.cn

logical changes of the flow field such as the transition from a single-connected domain to a multi-connected one, bubble merging and break, etc. It is also difficult for these methods to model the viscous effects of the fluids for flows with moderate Reynolds numbers, and are not convenient for giving the velocity and pressure distributions.

The other category is the kind of methods based on the full-flow-field solutions such as body-fitted grids methods,[9] front tracking methods,[10,11] level set methods,[12,13] volume of fluid (VOF) methods,[12,14−18] coupled level set and VOF (CLSVOF) methods,[19] etc. These methods can easily obtain the detailed velocity and pressure distributions as a direct result of the computations, can simulate viscosity effects on the flow, and some of them can easily track the topological changes of interfaces.

Among all those papers mentioned above, some of them (e.g. Ref. [19]) focused mainly on the numerical method and gave only the results but neglected the analysis of the mechanism of bubbles' behaviours. Others (e.g. Refs. [11] and [17]) did both simulation and mechanism analysis, nevertheless in these analyses, several factors such as the density ratio, the viscosity ratio, the Reynolds number and the Weber number were mixed, and the fluid mechanics and the bubble behaviour were not combined concretely, so that these analyses of the parametric effects are not accurate.

We are trying to analyse numerically the bubble deformation mechanism. The Weber number, the Reynolds number, the density ratio, and the viscosity ratio are the crucial dimensionless parameters for controlling the flow. In order to make a proper analysis, first we should study the effects of the four factors separately, and then study their combined effects, so that we can fully understand the associated mechanisms. In Ref. [20] we improved the VOF method and thereby we studied the mechanism of density ratio on the behaviour of a bubble or drop, and the mechanism of the generation of the liquid jet during the evolution of a bubble or drop, without taking into consideration the viscosity and surface tension effects.

As a succeeded work to Ref. [20], this paper will investigate numerically the surface tension effects on the behaviour of a rising bubble by the VOF method. The importance of surface tension is indicated by the Weber number We. Surface tension effects on the bubble behaviour can be important when the bubble size is very small, or when its curvature is large, or when the surface tension itself between two phases is huge. In a surface-tension-dominant two-phase flow field, the accurate calculation of the interface becomes a problem especially when the ratio of the gas density to the liquid density is very small. References [21] and [22] analysed numerically the mechanism of surface tension effect on the behaviour of the axisymmetric growth and collapse of one or two cavities near a solid wall by boundary integral method, but the numerical simulations were limited to the time before the transition to the toroidal bubble.

The remainder of this paper is arranged as follows. Section 2 gives the governing equations and numerical methods. Section 3 gives the numerical results and the mechanism analysis. Section 4 gives the conclusions.

2. Governing equations and numerical methods

We study the buoyancy-driven motion of an axisymmetric bubble with surface (abbreviated as S) in an infinite and initially stationary fluid. Let the fluids outside and inside S be marked by 1 and 2 respectively. The two fluids are assumed to be immiscible and incompressible. Let ρ and μ be the fluid density and viscosity respectively, and C the ratio of the volume of fluid 1 in a cell to the volume of the cell (C is called colour function). Let l_0, $u_0 = \sqrt{gl_0}$, $t_0 = l_0/u_0$, $p_0 = \rho_1 u_0^2$, ρ_1, and μ_1 be the reference quantities of length, velocity, time, pressure, density, and viscosity, respectively, and introduce the following dimensionless quantities

$$\bar{r} = r/l_0,\ \bar{z} = z/l_0,\ \bar{t} = t/t_0,\ \bar{u} = u/u_0,$$
$$\bar{v} = v/u_0,\ \bar{p} = p/p_0,\ \bar{\rho} = \rho/\rho_1,\ \bar{\mu} = \mu/\mu_1,$$

then we can obtain the dimensionless governing equations for the flow problem. In the above and following expressions, r and z are respectively the radial and axial coordinates, t is the time variable, u and v are respectively the r- and z-components of the velocity, p is the pressure, g is the acceleration due to gravity, σ is the surface tension between fluid 1 and 2, α is the total curvature of S, $\delta(S)$ is the Dirac δ-function with sources distributed on S, and n_r and n_z are respectively the r- and z-components of the unit normal of S. If we drop the sign '−' over any dimensionless quantity, then the dimensionless governing equations are

$$\frac{1}{r}\frac{\partial(ru)}{\partial r} + \frac{\partial v}{\partial z} = 0, \tag{1}$$

$$\frac{\partial u}{\partial t}+\frac{1}{r}\frac{\partial (ru^2)}{\partial r}+\frac{\partial (uv)}{\partial z}$$
$$=\frac{1}{\mathrm{We}\,\rho}\alpha\delta(S)n_r-\frac{1}{\rho}\frac{\partial p}{\partial r}+\frac{1}{\mathrm{Re}\,\rho}\left\{\frac{1}{r}\frac{\partial}{\partial r}\left(2\mu r\frac{\partial u}{\partial r}\right)+\frac{\partial}{\partial z}\left[\mu\left(\frac{\partial u}{\partial z}+\frac{\partial v}{\partial r}\right)\right]-\frac{2\mu u}{r^2}\right\}\ , \tag{2}$$

$$\frac{\partial v}{\partial t}+\frac{1}{r}\frac{\partial (ruv)}{\partial r}+\frac{\partial (v^2)}{\partial z}$$
$$=\frac{1}{\mathrm{We}\,\rho}\alpha\delta(S)n_z-\frac{1}{\mathrm{Fr}}-\frac{1}{\rho}\frac{\partial p}{\partial z}+\frac{1}{\mathrm{Re}\,\rho}\left\{\frac{1}{r}\frac{\partial}{\partial r}\left[r\mu\left(\frac{\partial u}{\partial z}+\frac{\partial v}{\partial r}\right)\right]+\frac{\partial}{\partial z}\left(2\mu\frac{\partial v}{\partial z}\right)\right\}\ , \tag{3}$$

$$\frac{\partial C}{\partial t}+u\frac{\partial C}{\partial r}+v\frac{\partial C}{\partial z}=0\ , \tag{4}$$

$$\rho=\lambda+C(1-\lambda)\ , \tag{5}$$

$$\mu=\beta+C(1-\beta)\ , \tag{6}$$

where the dimensionless parameters λ, β, Fr, Re, and We, are respectively the density ratio, viscosity ratio, Froude number, Reynolds number and Weber number, which are defined by

$$\lambda=\frac{\rho_2}{\rho_1}\ ,\quad \beta=\frac{\mu_2}{\mu_1}\ ,\quad \mathrm{Fr}=\frac{u_0^2}{gl_0},$$
$$\mathrm{Re}=\frac{\rho_1 u_0 l_0}{\mu_1},\quad \mathrm{We}=\frac{\rho_1 u_0^2 l_0}{\sigma}. \tag{7}$$

Because in this paper we take $u_0=\sqrt{gl_0}$, so we always have Fr = 1 and We $=\rho_1 g l_0^2/\sigma$ (in this case We is called Bond number B).

At the infinite boundary the velocity is set to zero and the pressure is set to the stationary fluid pressure. In the following computations, by making use of the axisymmetric property of the fluid flow, the grid points at the symmetric axis can be treated as inner grid points.

The governing equations are solved numerically by the method given in Ref. [20].

3. Numerical results

We will study the buoyancy-driven motion of an initially spherical bubble in another infinite and initially stationary fluid. In the non-dimensionalization, the reference length and velocity are taken to be R and $\sqrt{gR}$ respectively, where R is the radius of the bubble at $t=0$. Therefore, in the dimensionless system the radius of the bubble at $t=0$ is always 1, and the Froude number Fr is always 1. In this paper, all of the numerical results are in dimensionless form.

To solve our flow problem in infinite fluid, it is necessary to truncate the flow field to finite: $0\le r\le r_{\max}$ and $z_l\le z\le z_u$. Numerical experiments with $\Delta r=\Delta z=0.1$ show that when $r_{\max}\ge 3$ and d_l and d_u, the distances from the bubble to z_l and z_u, are greater than or equal to 2, the numerical results for the evolution of the bubble only have small differences for different $r_{\max}$, z_l and z_u. In the computations of this paper we take $r_{\max}=8$ and take values of z_l and z_u such that $d_l\ge 7$ and $d_u\ge 7$ are ensured during the evolution of the bubble. Numerical experiments also show that the numerical results obtained with $\Delta r=\Delta z=0.1$ and those with $\Delta r=\Delta z=0.2$ have distinguishable differences, but the numerical results with $\Delta r=\Delta z=0.1$ and those with $\Delta r=\Delta z=0.05$ only have small differences. Thus in the computations of this paper, we take $\Delta r=\Delta z=0.1$. In all of the computations, $\Delta t=0.001$ is used.

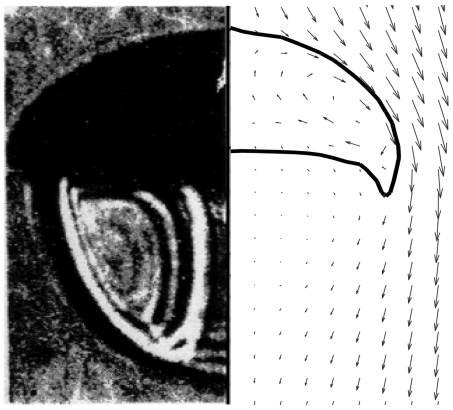

Fig. 1. Steady shape of the bubble and the corresponding flow pattern with $\lambda=0.0011$, $\beta=0.0085$, Re $=$ 9.8, We $=7.6$ and Fr $=0.76$. The left half is the results given in Ref. [6] and the right half is the present numerical results.

To demonstrate the correctness and validity of our method, figure 1 shows the comparison of our numerical results (the right half of the figure) with the experimental results (the left half) of Hnat and Buckmaster (Fig. 1(A) in Ref. [6]) for the case of $\lambda=0.0011$, $\beta=0.0085$, Re $=9.8$, We $=7.6$ and Fr $=0.76$. Figure 6 in Ref. [9] and Fig. 17 in Ref. [23] also gave similar comparisons. The terminal rise velocity measured in Ref. [6] is 21.5 cm/s, and that computed by our

method is 23.2 cm/s. It can be seen that the agreements in the steady shape of the bubble and the flow pattern between our result and that given in Ref. [6] are good.

For the case of $\lambda = 0.001$, $\beta = 0.01$, Re = 100, We = 200 and Fr = 1, figure 2(a) gives the evolution of an initially spherical gas bubble in a liquid obtained by our method, and figure 2(b) shows the corresponding result from Fig. 11 in Ref. [13] which was obtained by level set method. Quite good agreement is achieved except that the transition time to toroidal bubble is a little later in our result than that in Ref. [13]. For the case of $\lambda = 0.001$, Re $= \infty$, We = 10 and Fr = 1, figure 2 in Ref. [20] showed a very good agreement between our result and the result in Ref. [13]. Thus the correctness of our method is approved.

It has been known that in the inviscid and incompressible fluid flow frame and without taking consideration of surface tension effects, due to the action of the inertial force (i.e. the gradient of the pressure $p_{\rm df}$ that causes the bubble to deform, see Ref. [20]), two liquid jets will form during the rise of the bubble: one is large and behind the bubble, the other is much smaller and ahead of the bubble, and thus the development of the two jets will make the bubble toroidal.[20]

Now we investigate surface tension effects on the behaviour of a rising bubble in the inviscid fluid flow frame. It should be noted that for an initially spherical bubble the surface tension force will resist the increase of the area of the bubble surface and thus will resist the formation and development of the liquid jets. Therefore, whether or not the liquid jets will form, and if they form how they will develop and whether or not they cause the bubble to become toroidal, all these will depend on the relative importance between the inertial force and the surface tension force. In all of the computations the density ratio λ is set to 0.001, which is close to the case of an air bubble rising in the water.

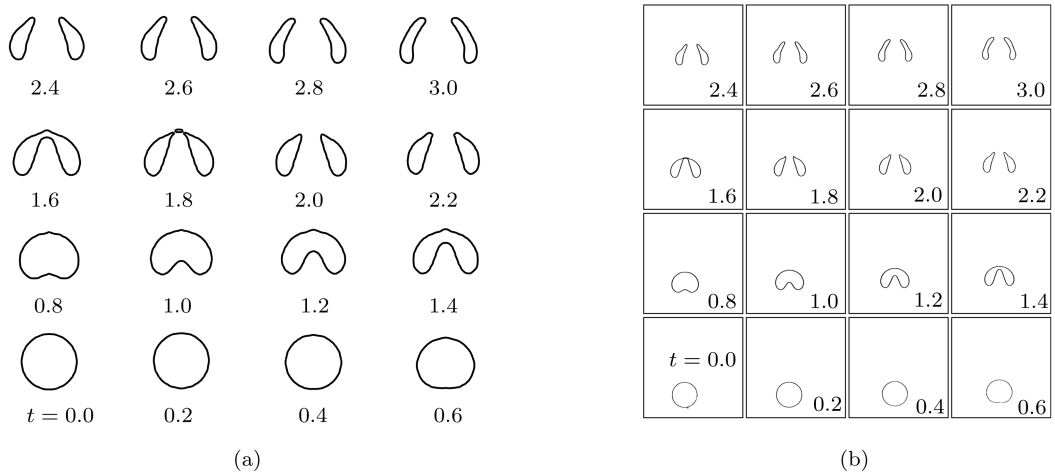

Fig. 2. Evolution of an initially spherical gas bubble in a liquid with $\lambda = 0.001$, $\beta = 0.01$, Re = 100, We = 200 and Fr = 1. (a) Result of this paper, and (b) result from Fig. 11 in Ref. [13].

For $\lambda = 0.001$, Re $= \infty$ and Fr = 1, figures 3(a)–3(h) give the evolution pictures of the bubble for We $= \infty$, 20, 8, 7, 5, 1.8, 1.7, and 1 respectively. The number below each picture indicates its corresponding time. It can be seen from Figs. 3(a)–3(h) that there exist four critical Weber numbers $\rm We_1$, $\rm We_2$, $\rm We_3$, and $\rm We_4$, which are between 1.7 and 1.8, 5 and 7, 7 and 8, and 20 and ∞, respectively. When We $>$ $\rm We_1$ the bubble will have the transition to toroidal form, and when We $<$ $\rm We_1$ the transition will not happen. When $\rm We_1 <$ We $<$ $\rm We_2$, the toroidal bubble will not break down into two toroidal bubbles and after the toroidal bubble evolves for a time, the radius at its top will become smaller and smaller and finally the bubble will return to simple-connected form. When We $>$ $\rm We_2$ the toroidal bubble will break down into two toroidal bubbles and the bubble will never return to the simple-connected form. When $\rm We_2 <$ We $<$ $\rm We_3$, after the toroidal bubble breaks down into two toroidal bubbles, the upper toroidal bubble will become simple-connected form. When We $>$ $\rm We_3$, after the toroidal bubble breaks down into two toroidal bubbles, the up-

per toroidal bubble will not become simple-connected. When $We > We_4$, during the evolution of the bubble, two liquid jets will form, one is large and behind the bubble and the other is much smaller and ahead of the bubble. When $We_1 < We < We_4$, only one liquid jet behind the bubble will form and the small liquid jet in front of the bubble will not appear. The mechanism of the last phenomenon is that when $We = \infty$, the interface curvature of the small liquid jet is large and the inertial force which causes the small liquid jet to form is small, therefore surface tension force is easy to resist the generation of the small liquid jet.

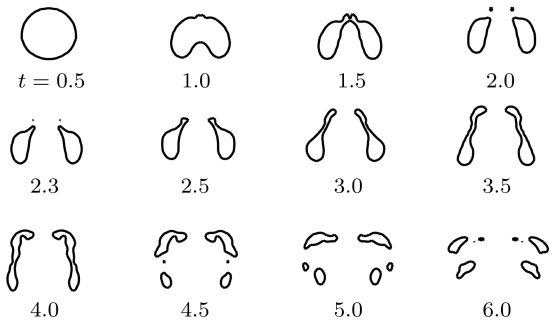

Fig. 3(a). The evolution of a gas bubble in liquid with $\lambda = 0.001$, $Re = \infty$, $We = \infty$ and $Fr = 1$.

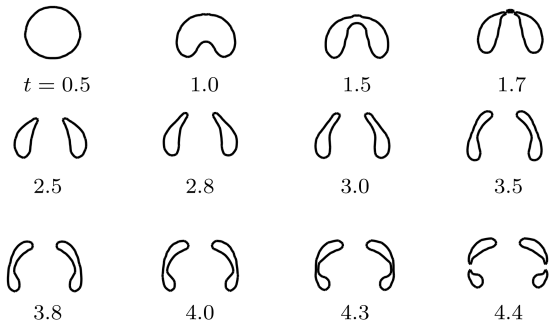

Fig. 3(b). The evolution of a gas bubble in liquid with $\lambda = 0.001$, $Re = \infty$, $We = 20$ and $Fr = 1$.

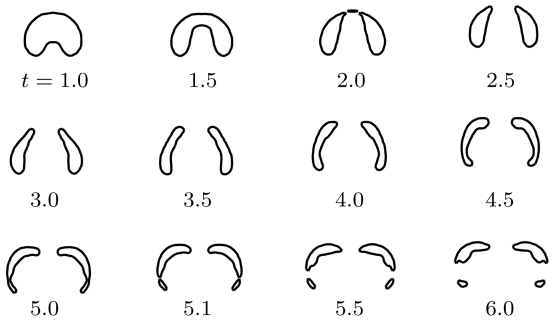

Fig. 3(c). The evolution of a gas bubble in liquid with $\lambda = 0.001$, $Re = \infty$, $We = 8$ and $Fr = 1$.

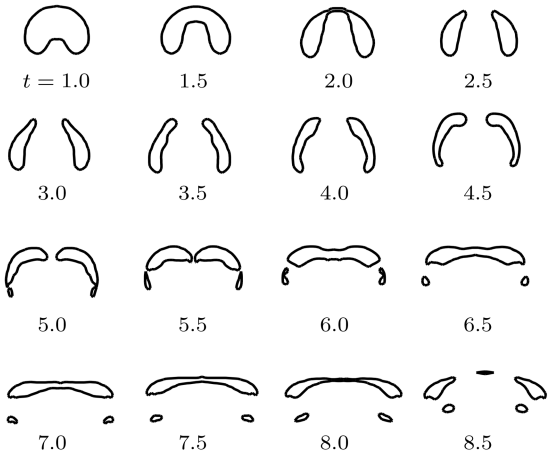

Fig. 3(d). The evolution of a gas bubble in liquid with $\lambda = 0.001$, $Re = \infty$, $We = 7$ and $Fr = 1$.

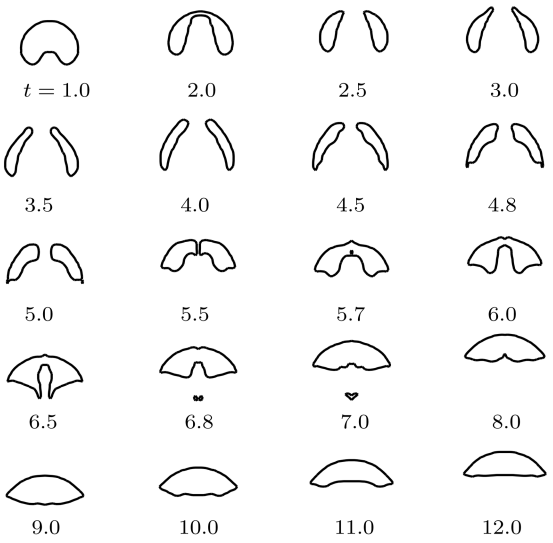

Fig. 3(e). The evolution of a gas bubble in liquid with $\lambda = 0.001$, $Re = \infty$, $We = 5$ and $Fr = 1$.

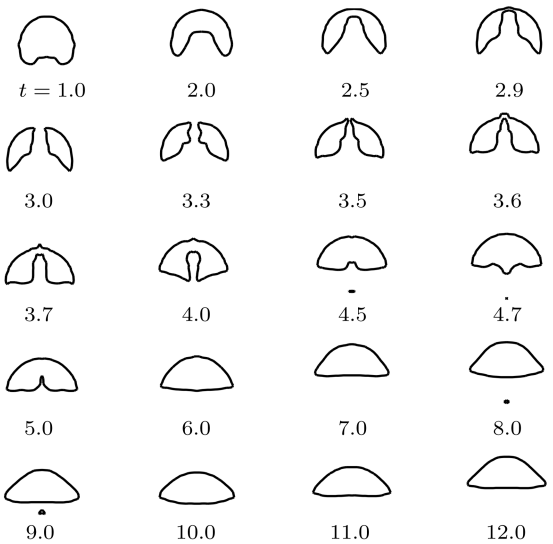

Fig. 3(f). The evolution of a gas bubble in liquid with $\lambda = 0.001$, $Re = \infty$, $We = 1.8$ and $Fr = 1$.

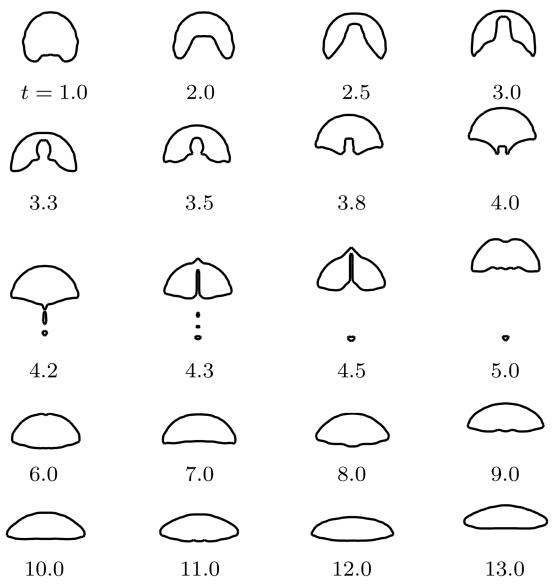

Fig. 3(g). The evolution of a gas bubble in liquid with $\lambda = 0.001$, $\mathrm{Re} = \infty$, $\mathrm{We} = 1.7$ and $\mathrm{Fr} = 1$.

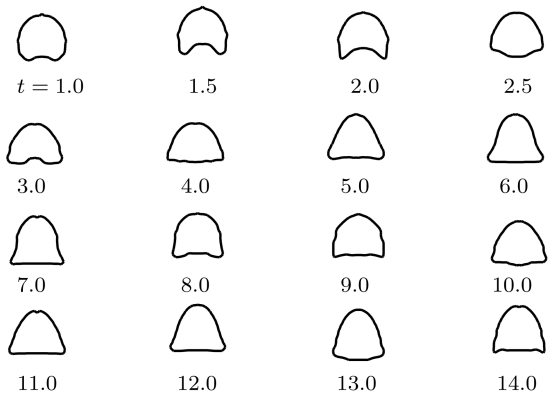

Fig. 3(h). The evolution of a gas bubble in liquid with $\lambda = 0.001$, $\mathrm{Re} = \infty$, $\mathrm{We} = 1$ and $\mathrm{Fr} = 1$.

It can be seen from Fig. 3(a) that in the case of inviscid fluid flow and without taking consideration of surface tension effects, after the toroidal bubble forms, it moves outward due to the action of the lift, and its section area decreases in order to keep the conservation of its volume. As was analysed in Ref. [20], the lift is induced by the co-action of the upward motion of the bubble and the circulation around its cross-section. The top becomes sharp and then the upper part of its section elongates and becomes thinner and thinner. Then the top of the toroidal bubble moves inward. Afterwards the lower part of the bubble becomes thinner and thinner. At the same time its upper part becomes a little fatter, its section continuously elongates upward and its top continuously moves inward. Then the lower middle part of the section becomes thinner and thinner, and finally the toroidal bubble breaks down into two toroidal bubbles. Now we analyse the mechanisms of the above phenomena. The outward motion of the liquid which is close to the bubble and inside the ring is much easier than that of the liquid which is outside the ring and close to the bubble. The reason is that the gas density is much lower than the liquid one, and thus the resistance to the inner liquid motion is much smaller than that to the outer liquid motion. In order to keep the conservation of the bubble volume, its section must elongate along axial direction. As shown in Fig. 4, the gradient of the pressure p_{df} below the bubble is much larger than that above the bubble so that the downward elongation of the section is much more difficult than the upward elongation of the section. Therefore the upper part of the section elongates and becomes thinner and thinner first. After the upper part of the section is thin enough, thinning becomes more and more difficult because the resistance to the outward motion of the liquid which is inside the ring and close to the upper part of the bubble increases. At this moment the lower part of the section is wider along the radial direction and thus is easier to become thin. Meanwhile, the gradient of p_{df} below the bubble is still much larger than that above the bubble, the downward elongation of the section is still difficult. Therefore the section continuously elongates upward and the gas moves upward, which causes the upper part of the section a little fatter. The mechanism of the inward motion of the top of the section is as follows. After the toroidal bubble forms, its section has an angle of attack along the upward direction. By Joukovsky moment of force theorem (Section 6.6 in Ref. [24]), the angle of attack will induce a moment of force which will in turn cause the increase of the angle of attack. This unstable process will continue until the angle of attack reaches $\pi/2$, the stable position of the section. Because the upper part of the section is thinner and thus has smaller moment of inertia, and because the gradient of p_{df} near this part is perpendicular to the direction of the rotation of the section and is much smaller than that of the liquid near the lower part, the rotation of the upper part is much easier than that of the lower part, which causes the inward motion of the top of the section.

It can be seen from Figs. 3(b)–3(f) that in the case of $\mathrm{We} > \mathrm{We}_1$, after the toroidal bubble forms, surface tension will resist the elongation of its upper part and make its surface smooth so that when the Weber number decreases, the upper part of its section will become thicker and thicker. Moreover, in

the case of We > We_2, when the Weber number decreases, the position where the toroidal bubble breaks down into two toroidal bubbles will move downward, so that after the toroidal bubble breaks down into two toroidal bubbles, the length of the section of the upper toroidal bubble will increase and consequently for the same section rotation angle, the distance of the inward movement of the top of the upper toroidal bubble will increase too.

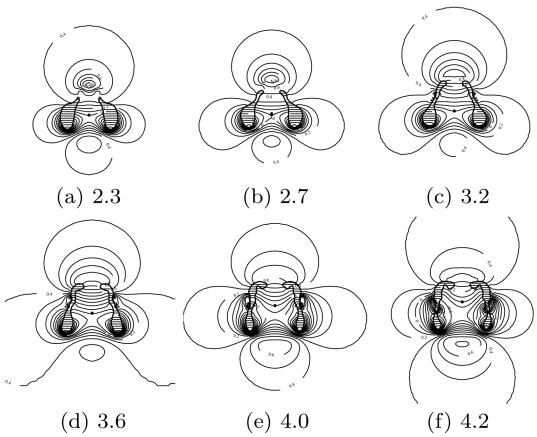

Fig. 4. The distribution of pressure $p_{\rm df}$ for $\lambda = 0.001$, Re = ∞, We = ∞ and Fr = 1.

It can be seen from Figs. 3(b)–3(d) that in the case of We > We_2, the inward motion of the top of the toroidal bubble will not stop until it breaks down into two toroidal bubbles, and after that, the inward motion of the top of the upper toroidal bubble will not stop until the section of the upper toroidal bubble reaches stable position, where the section is perpendicular to the axisymmetric axis. In the case of We > We_3, the radius of the top of the upper toroidal bubble is greater than zero when its section reaches stable position and therefore in this case the upper toroidal bubble will not become simple-connected. In the case of We_2 < We < We_3, the radius of the top of the upper toroidal bubble has decreased to zero before its section reaches stable position and thus in this case the upper toroidal bubble will become simple-connected.

It can be seen from Figs. 3(e) and 3(f) that in the case of We_1 < We < We_2, the inward motion of the top of the toroidal bubble will not stop until the radius of its top has decreased to zero and therefore in this case the bubble will return to simple-connected form.

It can be seen from Figs. 3(e)–3(h) that when the liquid jet begins to regenerate for the case of We_1 < We < We_2 or when the liquid jet stops to develop for the case of We < We_1 (although when We = 1 the jet is very short and wide), the velocity of the jet is zero and thus the inertial force acting on the jet is zero, and the surface tension force will pull the jet out of the bubble until the bottom of the bubble becomes flat where surface tension force is zero and the fluid velocity reaches its maximum and thus the inertial force also reaches its maximum. Then the inertial force will cause the bottom to move downward until the downward deformation of the bottom reaches its maximum. Then surface tension force will pull the bottom upward until the bottom becomes flat. Then the inertial force will push the bottom upward and thus a liquid jet forms again. This oscillation will not stop until the bubble reaches a steady shape. From this it can be seen that surface tension effects will dissipate the kinetic energy of the fluid (Ref. [24], Section 1.9), and thus damp the oscillation and make the bubble reach a steady form. During the oscillation some small bubbles caused by surface tension effects can occur at the surface with very large curvature.

It is known that for We > We_1 there will always be a liquid jet forming at the bottom of the bubble. Now we investigate the surface tension effects on the liquid jet. For $\lambda = 0.001$, Re = ∞ and Fr = 1, figure 5 gives the detailed evolution pictures of the bubble with We = ∞, 20 and 10. It can be seen that surface tension effects will resist the development of the liquid jet, reduce the curvature at the top of the jet, and delay the formation of the toroidal bubble.

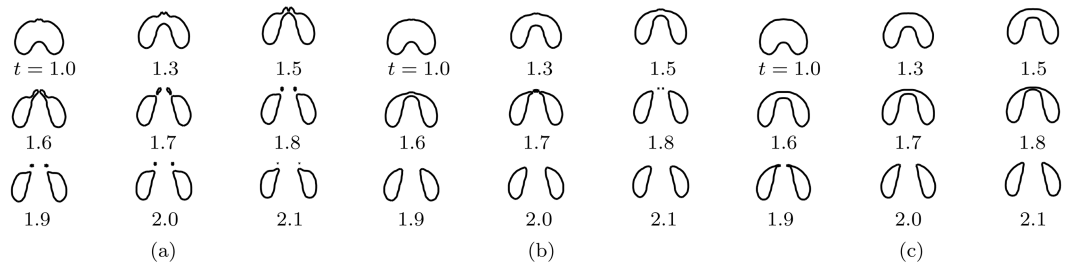

Fig. 5. The evolution of a gas bubble in liquid with $\lambda = 0.001$, Re = ∞ and Fr = 1. (a) We = ∞, (b) We = 20, (c) We = 10.

For $\lambda = 0.001$, Re $= \infty$, Fr $= 1$ and We $= 0.2$, figure 6 gives the evolution pictures of the bubble. It can be seen that the overall shape of the bubble will have oscillations: its axial and radial dimensions will stretch out and draw back alternatively; sometimes its top is much thinner than its bottom and sometimes its top is almost as wide as its bottom. Accompanying the oscillations, sometimes there occurs a very small liquid jet at the top or at the bottom of the bubble, and sometimes the jet disappears. As pointed out in Ref. [24] (Section 5.14), that only when the radius of the bubble is not greater than 0.05 cm (the corresponding Weber number is about 0.03), can the bubble remain approximately spherical. In the case of Fig. 6, the Weber number is not low enough to let the surface tension force totally suppress the action of the inertial force so that the bubble cannot keep a steadily spherical form.

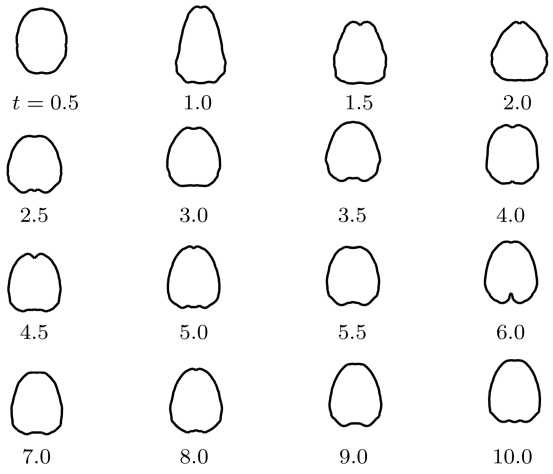

Fig. 6. The evolution of a gas bubble in liquid with $\lambda = 0.001$, Re $= \infty$, We $= 0.2$ and Fr $= 1$.

When $\lambda = 0.001$, Re $= \infty$, and Fr $= 1$, figure 7 shows the evolution of the centroid position of a gas bubble for different Weber numbers. It can be seen that for $1 \leq$ We $<$ We$_2$, i.e., when the bubble can finally reach a steady shape, after it rises acceleratedly for a moment, it will rise with an almost constant speed, and the lower the Weber number is, the higher the speed is. When We $>$ We$_2$, i.e., when the bubble cannot reach a steady shape, it will not rise with a constant speed. It is well known (Ref. [24], Section 6.4) that when a solid body is rising or falling in an inviscid liquid, it rises or falls acceleratedly with necessary consideration of additional mass of the body. The reason why a bubble can rise in an inviscid liquid with a constant speed is not clear. Perhaps in this case the dissipation effects caused by surface tension will, like the dissipation effects caused by viscosity, introduce a kind of drag which balances the buoyancy force.

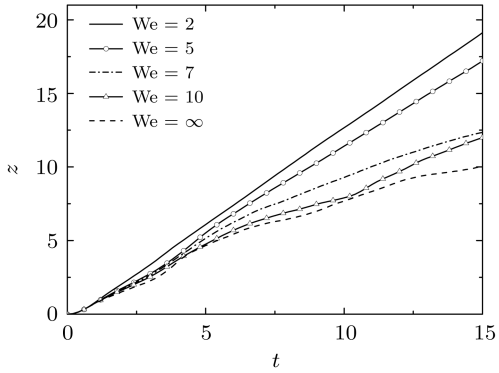

Fig. 7. Evolution of the centroid position of a gas bubble for different Weber numbers with $\lambda = 0.001$, Re$= \infty$, and Fr $= 1$.

4. Conclusions

In the inviscid and incompressible fluid flow regime, surface tension effects on the behaviour of an initially spherical buoyancy-driven bubble rising in an infinite and initially stationary liquid have been investigated numerically by a VOF method. The validity of the numerical method has been checked. It is found by numerical experiment that there exist four critical Weber numbers We$_1$, We$_2$, We$_3$, and We$_4$, which are between 1.7 and 1.8, 5 and 7, 7 and 8, and 20 and ∞, respectively. When We $>$ We$_1$ the bubble will have the transition to toroidal form, and when We $<$ We$_1$ the transition will not happen. When We$_1$ $<$ We $<$ We$_2$, the toroidal bubble will not break down into two toroidal bubbles and after the toroidal bubble evolves for a time the radius at its top will become smaller and smaller and finally the bubble will return to a simple-connected form. When We $>$ We$_2$ the toroidal bubble will break down into two toroidal bubbles and the bubble will never return to a simple-connected form. When We$_2$ $<$ We $<$ We$_3$, after the toroidal bubble breaks down into two toroidal bubbles, the upper toroidal bubble will become simple-connected. When We $>$ We$_3$, after the toroidal bubble breaks down into two toroidal bubbles, the upper toroidal bubble will not become single-connected. When We $>$ We$_4$, during the evolution of the bubble, two liquid jets will form, one is large and behind the bubble and the other is much smaller and ahead of the bubble. When We$_1$ $<$ We $<$ We$_4$ only one liquid jet behind the bubble will form and the small liquid jet in front of the bubble will not appear. Moreover,

after the liquid jet begins to regenerate for the case of $We_1 < We < We_2$, or for the case of $We < We_1$, due to the co-action of the inertial force and the surface tension force the bottom of the bubble will oscillate until the bubble reaches a steady shape. In the case of $We > We_1$, surface tension effects will resist the development of the liquid jet at the bottom of the bubble, reduce the curvature at the top of the jet and delay the transition to toroidal form. When the Weber number is quite low ($We = 0.2$), the overall shape of the bubble will have oscillations. It is also found that when $1 \leq We < We_2$, the bubble will finally reach a steady shape, and in this case after it rises acceleratedly for a moment, it will rise with an almost constant speed, and the lower the Weber number is, the higher the speed is. When $We > We_2$, the bubble will not reach a steady shape, and in this case it will not rise with a constant speed. The mechanism of the above phenomena has been analysed theoretically and numerically.

References

[1] Moore D W 1959 *J. Fluid Mech.* **6** 113
[2] Taylor T D and Acrivos A 1964 *J. Fluid Mech.* **18** 466
[3] Davies R M and Taylor F I 1950 *Proc. R. Soc. Lond.* A **200** 375
[4] Walters J K and Davidson J F 1962 *J. Fluid Mech.* **12** 408
[5] Walters J K and Davidson J F 1963 *J. Fluid Mech.* **17** 321
[6] Hnat J G and Buckmaster J D 1976 *Phys. Fluids* **19** 182
[7] Bhaga D and Weber M E 1981 *J. Fluid Mech.* **105** 61
[8] Zhang Y L, Yeo K S, Khoo B C and Wang C 2001 *J. Comp. Phys.* **166** 336
[9] Ryskin G and Leal L G 1984 *J. Fluid Mech.* **148** 19
[10] Unverdi S O and Tryggvason G 1992 *J. Comp. Phys.* **100** 25
[11] Hua J S and Jing L 2007 *J. Comp. Phys.* **222** 769
[12] Liu R X and Shu C W 2003 *Some New Methods in Computational Fluid Dynamics* (Beijing: Science Press) (in Chinese)
[13] Sussman M and Smereka P 1997 *J. Fluid Mech.* **341** 269
[14] Hirt C W and Nichols B D 1981 *J. Comp. Phys.* **39** 201
[15] Rider W J and Kothe D B 1998 *J. Comp. Phys.* **141** 112
[16] Zou J F, Huang Y Q, Ying X Y and Ren A L 2002 *China Ocean Engnrg.* **16** 525
[17] Chen L and Suresh V 1999 *J. Fluid Mech.* **387** 61
[18] Wan D C 1998 *Chinese J. Comp. Phys.* **15** 655
[19] Sussman M 2003 *J. Comp. Phys.* **187** 110
[20] Wang H, Zhang Z Y, Yang Y M, Hu Y and Zhang H S 2008 *Chin. Phys.* B **17** 3847
[21] Zhang Z Y and Zhang H S 2004 *Phys. Rev.* E **70** 056310
[22] Zhang Z Y and Zhang H S 2005 *Phys. Rev.* E **71** 066302
[23] Sussman M, Smith K M, Hussaini M Y, Ohta M and Zhi-Wei R 2007 *J. Comp. Phys.* **221** 469
[24] Batchelor G K 1967 *An Introduction to Fluid Dynamics* (Cambrndge: Cambridge University Press) Section 1.9, 5.14, 6.4, 6.6